Desalination and Water Treatment
www.deswater.com

doi: 10.1080/19443994.2016.1157762

57 (2016) 25848–25856
November

Taylor & Francis
Taylor & Francis Group

Photocatalytic degradation of *p*-nitrophenol and methylene blue using Zn-TCPP/Ag doped mesoporous TiO_2 under UV and visible light irradiation

Mahboubeh Rabbani*, Hamideh Bathaee, Rahmatollah Rahimi, Ali Maleki

Department of Chemistry, Iran University of Science and Technology, Narmak, Tehran 16846-13114, Iran, Tel. +98 21 77240561; Fax: +98 21 77491204; email: m_rabani@iust.ac.ir (M. Rabbani), Tel. +98 21 77240516; Fax: +98 21 77491204; email: h.bathaee@yahoo.com (H. Bathaee), Tel. +98 21 77240290; Fax: +98 21 77491204; email: rahimi_rah@iust.ac.ir (R. Rahimi), Tel. +98 21 77240516; Fax: +98 21 77491204; email: maleki@iust.ac.ir (A. Maleki)

Received 5 December 2014; Accepted 17 February 2016

ABSTRACT

In this study, Ag-doped mesoporous TiO_2 powder was prepared via a sol–gel route with Pluronic P123 as template and then was modified with zinc(II) tetrakis(4-carboxyphenyl)-porphyrin. The catalysts were characterized by X-ray diffraction, diffuse reflectance spectroscopy, Fourier transform infrared (FT-IR), scanning electron microscopy, N_2 sorption experiments (BET), X-ray fluorescence analysis, and inductively coupled plasma spectroscopy. The photocatalytic activities of Ag-doped mesoporous TiO_2 and Zn-TCPP/Ag-doped mesoporous TiO_2 were evaluated using methylene blue and *p*-nitrophenol as pollutant compounds under UV and visible light irradiation. The results show that Zn-TCPP/Ag-doped mesoporous TiO_2 have higher activity than Ag-doped mesoporous TiO_2 under visible light irradiation, but its activity is lower under UV light irradiation.

Keywords: Zn-TCPP; Ag-doped TiO_2; Photocatalytic activity, *p*-Nitrophenol (PNP); Methylene blue (MB); Light irradiation

1. Introduction

In the last years, a big concern about the environment has emerged. *p*-nitrophenol (PNP) is an organic pollutant that is most widespread in the aqueous environment, due to their high solubility and stability in water [1,2]. It has been used extensively as a raw material in chemical industry for the manufacture of pesticides, herbicides, synthetic dyes, and pharmaceuticals, and for leather treatment and military [3]. Methylene blue (MB) is a heterocyclic aromatic chemical compound that has many uses in a range of different fields [4]. Due to environmental hazard, MB and PNP must be removed from aqueous environment.

There are common purification techniques for them including combustion, adsorption, biological treatment, and air stripping among which the advanced oxidation processes (AOPs) have been extensively utilized for the decomposition of hazardous or recalcitrant pollutants in the environment [5]. Analogously to other AOPs, the radiation technology employs very reactive species, primarily hydroxyl radicals (·OH), produced by water radiolysis for the decomposition of toxic or refractory organic compounds [6].

In the past decades, scientists and engineers are all interested in developing the semiconductor

*Corresponding author.

photocatalytic reactions. TiO_2 has widely been investigated for photocatalyzed degradation of organic dyes because of its high photoactive ability, stability, non-toxic, and low cost [6–11].

TiO_2 photocatalyst is well known to generate various active oxygen species such as hydroxyl radicals, hydrogen peroxide, and superoxide radical anions by redox reactions under UV irradiation. Anatase-type of TiO_2 has highly photocatalytic activity for decomposition of various environmental pollutants in both gas and liquid phases [12–19].

However, TiO_2 can only utilize energy of ultraviolet (UV) light (less than 5%) of the solar light energy for photocatalytic oxidation, whereas 97% of the visible spectra of sunlight reaching the surface of earth are unable to be used by TiO_2 [20]. In order to achieve photo-oxidation of pollutants with efficient utilization by titania particles under visible light irradiation, i.e. the band gaps must be smaller than 3.2 eV, the development of photocatalysts with high activity under visible light irradiation has been required. Thus, extensive researches have been conducted to convert the TiO_2 absorption from the ultraviolet to the visible light region by the ion doping of transition metals [21]. Among these transition metals, Ag has received much attention because its introduction can excellently extend the visible light absorption.

In other hand, porphyrin is a purple ampholine. To date, the greatest application of porphyrin dye is utilized on the titanium-based dye-sensitized solar cells (DSSCs) [22]. However, it is rarely applied on the study of environmental pollutant treatment [23,24].

In present work, Ag-doped mesoporous TiO_2 was synthesized using P123 as a surfactant by sol–gel approach and then was modified with zinc(II) tetrakis (4-carboxyphenyl)porphyrin (Zn-TCPP). The photocatalytic degradation of methylene blue (MB) and *p*-nitrophenol (PNP) using Zn-TCPP/Ag-doped mesoporous TiO_2 was evaluated under UV and visible light irradiation.

2. Experimental

2.1. Materials and methods

All of the chemicals used in this work were analytical grade reagents and used without further purification. Deionized water was used to prepare all solutions.

X-ray diffraction (XRD) analysis was performed on a D Jeoljdx-8030 X-ray powder diffractometer with Cu K_α (l = 0.154 nm) radiation (40 kV, 30 mA). To estimate the average crystallite sizes of Ag–TiO_2 NPs, the Scherrer equation was applied. Furthermore, the amount of immobilized metalloporphyrin and Ag doped on TiO_2 was determined by X-ray fluorescence analysis (XRF) analysis and inductively coupled plasma (ICP) spectroscopy. The particle morphologies of the as-prepared powders were observed by a Hitachi scanning electron microscopy (SEM) at 30 kV. The Fourier transform infrared (FT-IR) analyses were carried out on a Shimadzu FTIR-8400S spectrophotometer using a KBr pellet for sample preparation. Surface areas and pore size distribution were determined using Brunauer–Emmett–Teller (BET) multilayer nitrogen adsorption method in a conventional volumetric technique by ASAP 2020 micromeritics instrument. The diffuse reflectance spectroscopy (DRS) spectra were prepared via a Shimadzu (MPC-2200) spectrophotometer. For investigation of photocatalytic ability of nanocatalysts, the concentration of pollutant solutions was determined spectrophotometrically using a double-beam UV–visible spectrometer (Shimadzu UV-1700) at room temperature in the range of 200–800 nm.

2.2. Preparation of Ag-doped mesoporous TiO_2 (Ag–TiO_2)

The Ag-doped mesoporous TiO_2 nanoparticles were prepared by sol–gel synthesis in water medium. In a typical synthesis, the amount of 1.86 mL concentrated HCl and 0.02 g $AgNO_3$ was added to the conic flask containing 50 mL of deionized water (pH 1–2). Then, a solution contain 30 mL of titanium tetraisopropoxide (TTIP) and 20 mL ethanol was added drop by drop to the water–acid mixture under continuous stirring at the temperature of 50˚C. The white and dense precipitate was formed and gradually peptized after 3 h to form a transparent sol. Then, the obtained sol was dosed with 3 g of a template Pluronic P123, leading to the formation of a gel which was dried in the air at the temperature of 60˚C. The dried sample was calcined at the temperature of 400˚C for 4 h in air at the heating rat of 2˚C/min to remove the surfactant. For comparison, pure TiO_2 was prepared according to above process except adding $AgNO_3$.

2.3. Preparation of zinc(II) tetrakis(4-carboxyphenyl)porphyrin (Zn-TCPP)

The TCPP was synthesized according to the method of Adler [16], 2.33 mmol pyrrole and 2.33 mmol 4-carboxybenzaldehyde were refluxed in 100 mL of propionic acid for 4 h. The purification of product was done by column chromatography following the literature procedure. To prepare Zn-TCPP, 1 mmol TCPP and 2 mmol $Zn(Ac)_2$ were dissolved in 70 mL DMF and refluxed at 155˚C for 6 h.

2.4. Preparation of Zn-TCPP/Ag-doped mesoporous TiO_2 (Zn-TCPP/Ag-TiO_2)

0.5 g of the above-prepared TiO_2 powder and 0.05 g Zn-TCPP were added into DMF solvent and the mixed solution was refluxed for 5 h at 155˚C. Then, the prepared solid filtered and washed by DMF and water several times.

2.5. Investigations of photocatalytic properties

Fifty milliliters of MB and PNP with a known initial concentration and 0.05 g of the catalyst NPs were added to a Pyrex glass photoreactor. A 500 W high-pressure Hg lamp and a 500 W tungsten lamp were used as UV and visible light irradiation sources, respectively. Reaction solution was sonicated for 4 min to obtain a homogeneous suspension and then was magnetically stirred in the dark for 1 h to establish a MB and PNP adsorption/desorption equilibrium. During irradiation, the reaction medium was continuously purged with air at a constant flow rate to guarantee sufficient O_2 concentration in it. Samples of 2 mL were collected from supernatant solution every 30 min ones and immediately centrifuged at 14,000 rpm for 20 min. For investigation of photocatalytic ability of nanocatalysts, the concentration of MB and PNP was determined spectrophotometrically using a double-beam UV–visible spectrometer (Shimadzu UV-1700) at room temperature in the range of 200–800 nm.

The reusability and stability of the heterogeneous catalyst were studied for four times. In order to reuse the catalyst, after reaction completion, the catalyst was separated by centrifuging, then washed 3 times with ethanol and acetone, and then heated at 60˚C for 8 h. The recycled catalyst was applied for subsequent run. The recycled catalysts were used in the fresh reaction under the same reaction conditions.

3. Result and discussion

3.1. The XRD pattern

The powder XRD pattern (2θ range from 4˚ to 90˚) of the synthesized Ag-doped mesoporous TiO_2 and Zn-TCPP/Ag-doped mesoporous TiO_2 samples were shown in Fig. 1. The diffraction peaks at $2\theta = 25.33$˚, 37.75˚, 47.95˚, 54.13˚, and 62.72˚ corresponding to the anatase phase of titania (JCPDS, file no. 21-1272) are observed in the sample that displayed pure anatase phase. The average crystallite size calculated by Scherrer equation is 21 nm for Ag-doped mesoporousTiO_2 particles. The XRD spectra of Zn-TCPP/Ag-doped mesoporous TiO_2 are similar to the XRD spectra of Ag-TiO_2; however, the intensity of its peaks decreases rather than Ag-TiO_2.

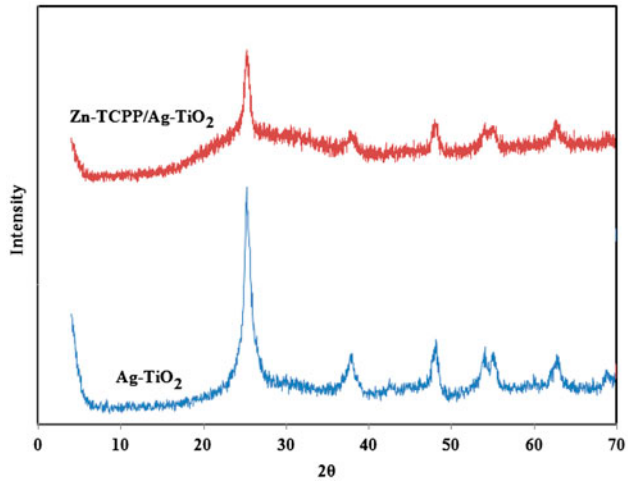

Fig. 1. The XRD pattern of Ag-doped mesoporous TiO_2 and Zn-TCPP/Ag-doped mesoporous TiO_2 photocatalyst.

3.2. Elemental analysis

The quantitative analysis of Ag doped into TiO_2 and metalloporphyrin loading on the surface of Ag–TiO_2 catalyst was estimated using XRF and ICP techniques. The obtained results from two techniques were relatively same and have been summarized in Table 1. As shown in this Table, the percentage of Ag doped into TiO_2 was 0.092% and the amount of Zn in TCPP/Ag-TiO_2 composite was 0.461%. The molecular weight of $ZnC_{48}H_{30}N_4O_8$ is 856.17; therefore, the obtained amount of metalloporphyrin loaded on the surface of Ag-TiO_2 catalyst was 4.8 1%.

3.3. The FT-IR spectra

The FT-IR spectra of the Zn-TCPP/Ag-TiO_2 and Ag-TiO_2 are shown in Fig. 2. The peaks at 3,420–3,450 cm^{-1} and 1,630–1,640 cm^{-1} were assigned to the stretching vibration and bending vibration of surface –OH group and the band at 520–580 cm^{-1} was

Table 1
The elemental analysis of Ag–TiO_2 and Zn-TCPP/Ag–TiO_2

Catalyst	Ti (%)	Ag (%)	Zn (%)
Ag-TiO_2	99.908	0.092	–
Zn-TCPP/Ag-TiO_2	99.450	0.089	0.461

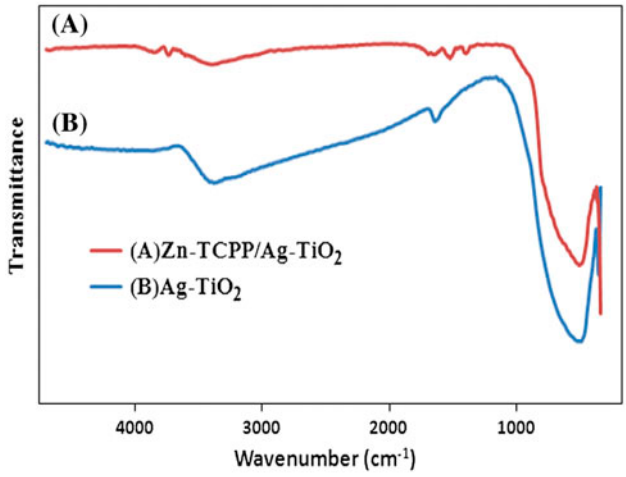

Fig. 2. The FT-IR spectra of (A) Zn-TCPP/Ag-doped mesoporous TiO_2 and (B) Ag doped mesoporous TiO_2.

assigned to the Ti–O and Ag–O stretching vibration. The strong C=O stretching band can be observed at 1,720 cm^{-1} in the IR spectrum of ZnTCPP/Ag-TiO_2. Two weak peaks appear at 1,630 and 1,380 cm^{-1} can be assigned to the antisymmetric and symmetric stretch of $–COO^-$. Therefore, the Zn-TCPP molecules should be chemisorbed on the surface of TiO_2 nanoparticles through O=C–O–Ti bonds, which can also enhance the electron transfer between Zn-TCPP and Ti (3d) orbital manifold of TiO_2, and further lead to the delocalization of π^* orbits of Zn-TCPP. Correspondingly, the energy of the π^* orbits of Zn-TCPP strong C=O stretching band can be observed at 1,692 cm^{-1} in the IR spectrum of pure Zn-TCPP [25].

3.4. The SEM images

The surface morphological study of the TiO_2 photocatalysts was carried out using SEM image. Fig. 3 shows the SEM image of the Zn-TCPP/Ag-doped mesoporous TiO_2 and Ag-doped mesoporous TiO_2 nanoparticles. It can be seen that the size of the TiO_2 is in the range of nanometer (30–50 nm). The average of nanoparticles was measured by Digimizer image analysis software.

3.5. Nitrogen adsorption–desorption

To give out the better understanding of the pore structure of Ag-doped mesoporous TiO_2 and Zn-TCPP/Ag-doped mesoporous TiO_2 materials, the nitrogen adsorption–desorption analysis performed at 77 K. Before the analysis, the materials were degassed by heating with evacuation at 453 K for 180 min to eliminate the contaminations. Adsorption–desorption isotherms for Ag-doped mesoporous TiO_2 and Zn-TCPP/Ag-doped mesoporous TiO_2 are shown in Fig. 4(A).

The corresponding isotherms show type IV isotherm in the IUPAC classification, characteristic of mesoporous materials. From the two branches of adsorption–desorption isotherms, the presence of a sharp adsorption step in the P/P_0 region from 0.4 to 0.8 and a hysteresis loop at the relative pressure $P/P_0 > 0.4$ show that the materials possess a well-defined array of regular mesopores. These isotherms therefore show that the materials possess good mesostructural ordering and a narrow pore size distribution. Pore size distribution curves are shown in Fig. 4(B).

Table 2 summarizes the results of N_2 adsorption analyses. After incorporation of porphyrin into Ag-TiO_2, the S_{BET}, V_t, and D_{BJH} values were 60.1722 $m^2\,g^{-1}$, 0.1591 $cm^3\,g^{-1}$, and 6.116 nm, respectively, whereas for neat Ag–TiO_2 were 69.2905 $m^2\,g^{-1}$, 0.1686 $cm^3\,g^{-1}$, and 6.896 nm, respectively. Therefore, all parameters of Zn-TCPP/Ag–TiO_2 decreased compared with neat Ag–TiO_2. This is fully consistent with the results of the XRD, FT-IR, and UV–vis studies and confirms that the porphyrin was successfully incorporated into the pores of Ag–TiO_2.

3.6. DRS spectra

Fig. 5 shows the DRS-UV–vis absorption spectra and band gap of Ag–TiO_2, Zn-TCPP/Ag–TiO_2, and pure TiO_2. It is obvious from Fig. 5(A) and (B) that the doped Ag can improve the absorption of mesoporous TiO_2 in the visible light region. This extended absorbance indicates the possible enhancement in the photocatalytic activity of mesoporous TiO_2 illuminate by visible light. The gap band of Ag-TiO_2 and pure TiO_2 was 3.28 and 3.45 eV, respectively.

The UV–vis-DRS absorption spectra of Zn-TCPP/Ag-TiO_2 are shown in Fig. 5(C). It is known that absorption spectra of Zn-TCPP in ethanol solution have a sharp peak around 400 nm (the Soret band) and four distinct peaks in the visible region (the Q-bands) centered at 513, 546, 588, and 645 nm, respectively, while for the Zn-TCPP/Ag–TiO_2, all of these bands absorption observed was red-shifted. The shift values can be due to interaction of porphyrin molecules with Ag–TiO_2 or J-aggregates of Zn-TCPP molecules chemisorbed on mesoporous TiO_2 [26].

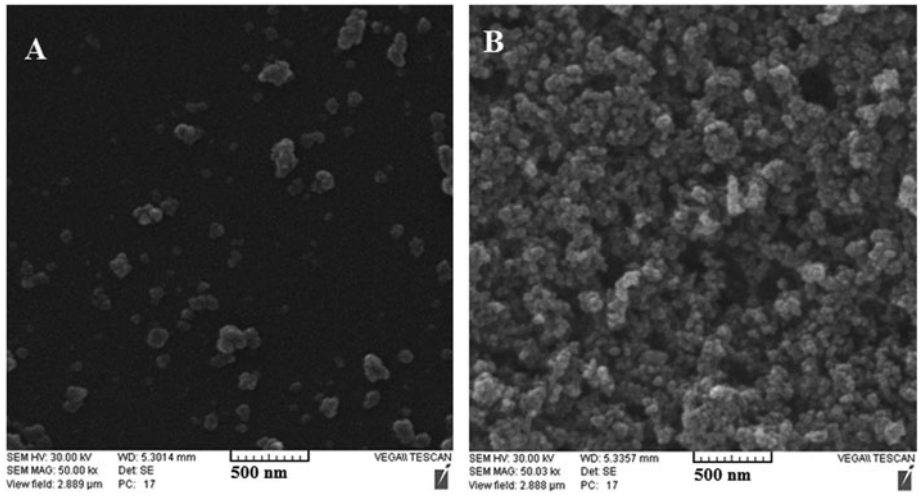

Fig. 3. The SEM image of (A) Zn-TCPP/Ag-doped mesoporous TiO_2 and (B) Ag doped mesoporous TiO_2.

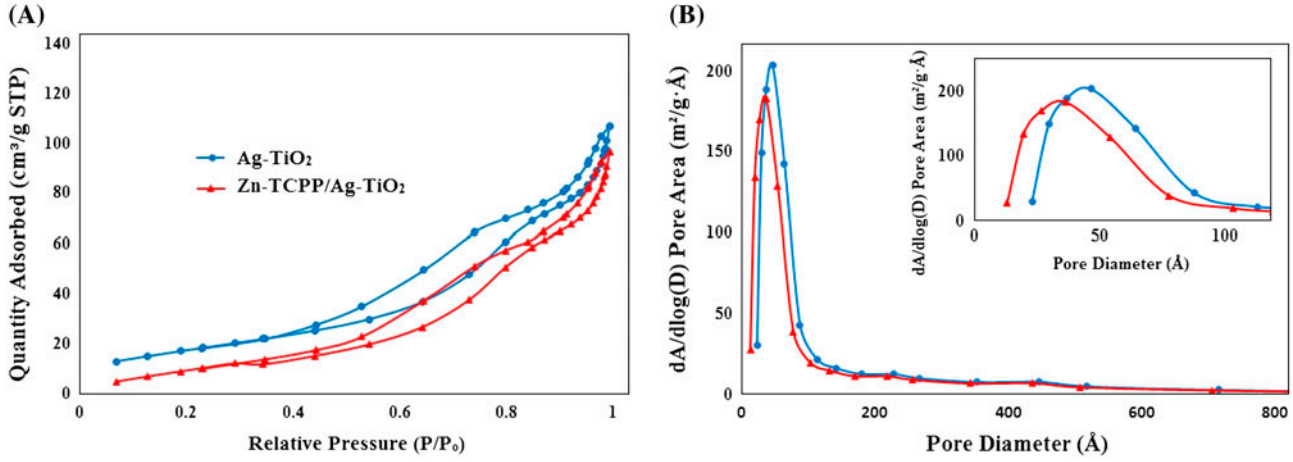

Fig. 4. (A) N_2 adsorption–desorption and (B) pore distribution of Ag-doped mesoporous TiO_2 and Zn-TCPP/Ag-doped mesoporous TiO_2.

Table 2
Textural properties from N_2 adsorption–desorption isotherm measurement of characteristics of Ag–TiO_2 and Zn-TCPP/Ag–TiO_2

Sample	BET surface area ($m^2\ g^{-1}$)	V_t ($cm^3\ g^{-1}$)	D_{BJH} (nm)
Ag-TiO_2	69.2905	0.1686	6.896
Zn-TCPP/Ag-TiO_2	60.1722	0.1591	6.116

3.7. Photocatalytic activity

The photocatalytic activity of Ag–TiO_2 and Zn-TCPP/Ag–TiO_2 catalysts under visible and UV light irradiation was defined by measuring the photodegradation of MB and PNP aqueous solutions. MB and PNP have different molecular structures and different functional groups: Methylene blue is a cationic dye with a methyl nitride group [$(CH_3)_2\ N^+$] and *p*-nitrophenol is an organic pollutant with hydroxyl and nitro groups.

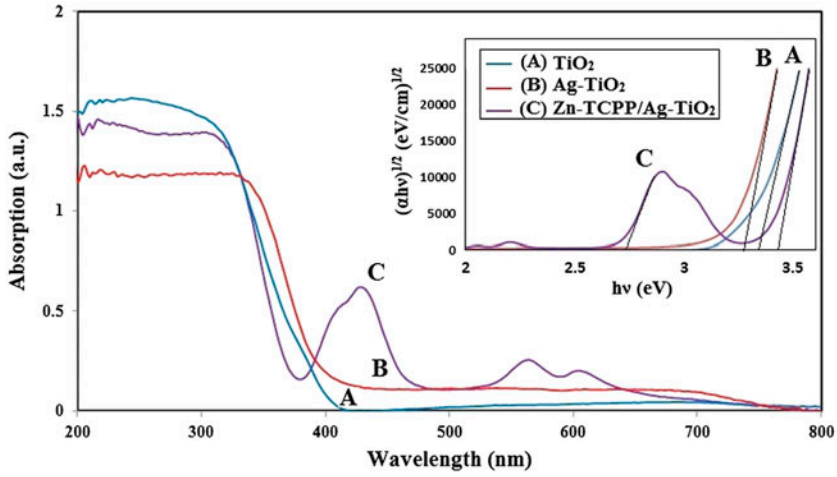

Fig. 5. The UV–vis diffuse reflectance spectra and (in inset) band gap of (A) pure TiO_2, (B) Ag-TiO_2 and (C) Zn-TCPP/Ag-TiO_2.

Fig. 6 shows the degradation of MB (5 mg L^{-1}) in the presence of Ag–TiO_2 and Zn-TCPP/Ag–TiO_2 catalysts under UV light irradiation. The Ag–TiO_2 catalyst exhibited better degradation of MB rather than Zn-TCPP/Ag–TiO_2 in this condition because Ag–TiO_2 has high gap band (3.28 eV) and therefore it activate under high energy UV light irradiation. On the other hands, the presence of porphyrin onto its surface can be led to decrease in active sites to uptake UV light that cause decrease in it photodegradation activity.

The photodegradation of MB and PNP (concentrations of 5 and 10 mg L^{-1}) in the presence of Ag–TiO_2 and Zn-TCPP/Ag–TiO_2 catalysts was investigated under visible light irradiation too. Fig. 7(A)–(D) display the plots of time dependence on the unconverted fraction (C/C_0) by different catalysts Ag–TiO_2 and Zn-TCPP/Ag–TiO_2 under UV and visible light irradiation. The comparison of curves shows that the best photocalytic efficiency obtained in presence of Ag–TiO_2 catalyst under UV light irradiation because the bang gap of Ag–TiO_2 is in range of ultraviolet. But under visible light irradiation, Zn-TCPP/Ag–TiO_2 was the better catalyst due to the presence of porphyrin as an antenna to collect the visible light. However, the activity of both catalysts is higher under UV light rather than visible light.

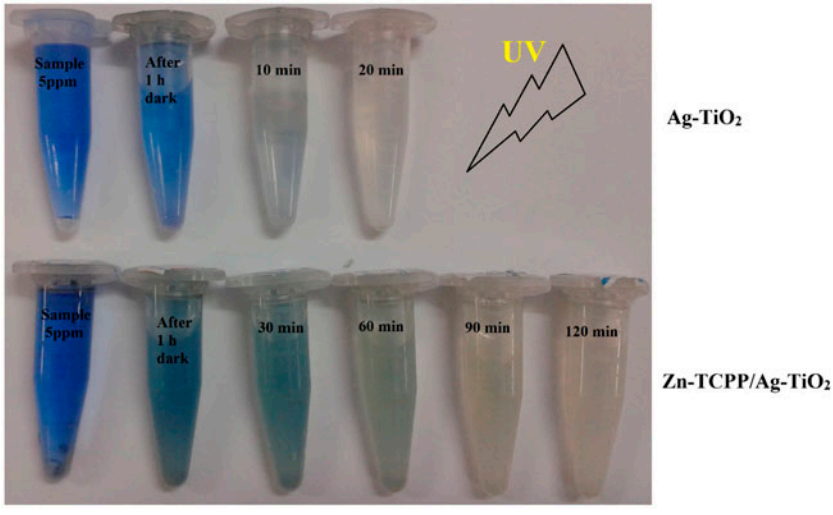

Fig. 6. The photocatalytic degradation of MB (5 mg L^{-1}) in presence of (A) Zn-TCPP/Ag doped mesoporous TiO_2 and (B) Ag-doped mesoporous TiO_2 under UV light irradiation.

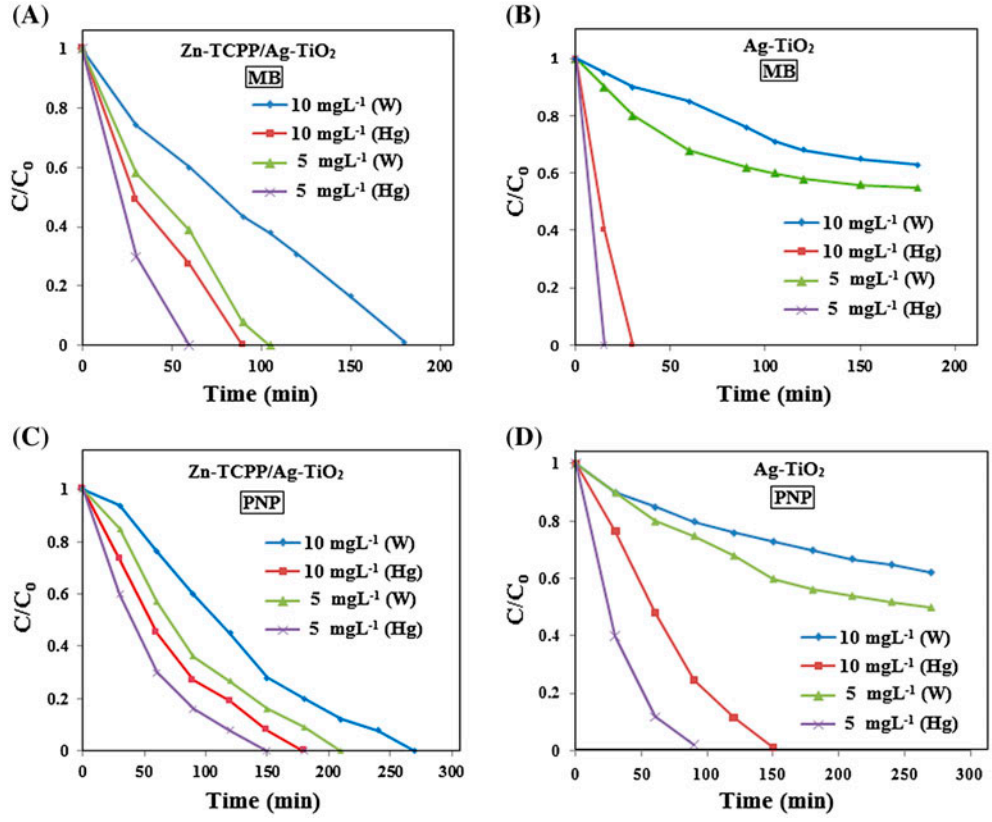

Fig. 7. The plots of time dependence on the unconverted fraction (C/C_0) for photocatalytic degradation of MB by (A) Zn-TCPP/Ag-doped mesoporous TiO_2 and (B) Ag-doped mesoporous TiO_2 and the photocatalytic degradation of PNP by (C) Zn-TCPP/Ag-doped mesoporous TiO_2 and (D) Ag-doped mesoporous TiO_2 under UV and visible light irradiation (conditions: 50 mL of 5 and 10 mg L^{-1} concentrations and 0.05 g catalyst).

The removal efficiencies of MB and PNP (concentrations of 5 and 10 mg L^{-1}) in the presence of TiO_2, Ag–TiO_2, and Zn-TCPP/Ag–TiO_2 catalysts under UV and visible light irradiation for 30 min are compared in Fig. 8. As can be seen, under UV irradiation, the photodegradation by Ag–TiO_2 is better photocatalyst, but under visible light irradiation, photodegradation by Zn-TCPP/Ag–TiO_2 is better.

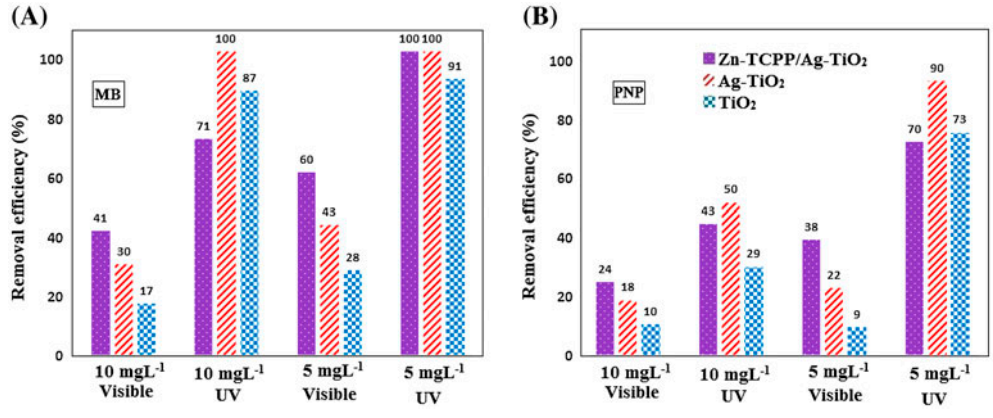

Fig. 8. Removal efficiency of photodegradation of (A) MB and (B) PNP in the presence of TiO_2, Ag–TiO_2 and Zn-TCPP/Ag–TiO_2 under UV and visible light irradiation (conditions: 50 mL of 5 and 10 mg L^{-1} concentrations, 0.05 g catalyst, 60 min).

3.8. Mechanism

A possible mechanism for degradation of organic pollutants by Zn-TCPP/Ag-TiO_2 under visible light irradiation is shown in Fig. 9. The porphyrin and doped Ag can increase the efficiency of photodegradation due to excitation at visible region. Once an excitation photon is absorbed, a single molecule Zn-TCPP is easily excited from S_0 ground state to the S_1 excited state. The generated electron injected into the conduction band (CB) of Ag–TiO_2, owing to the CB level of Ag–TiO_2, is near the LUMO of porphyrin. On the other hand, the electrons in the valence band (VB) of Ag-TiO_2 are preferentially excited to its CB thus generate an equal amount of holes in its VB. The photogenerated holes transfer from the VB of Ag–TiO_2 to the HOMO of porphyrin. Therefore, the probability of electron–hole recombination can be reduced. The accumulated electrons in the CB and the holes on the porphyrin surface can produce hydroxyl radicals from H_2O and dissolved O_2 that effectively promote oxidation reaction. Finally, derived hydroxyl radicals decompose MB or PNP to carbon dioxides and water.

3.9. Catalyst reusability

For investigation of reusability of Zn-TCPP/Ag–TiO_2 catalyst, after reaction completion, the catalysts were separated, then washed several times with acetone and ethanol, and dried before reusing in another photocatalytic degradation reaction. The results of reusability experiment (Fig. 10) showed that catalyst was reused for four times and no significant change was observed in photocatalytic activity.

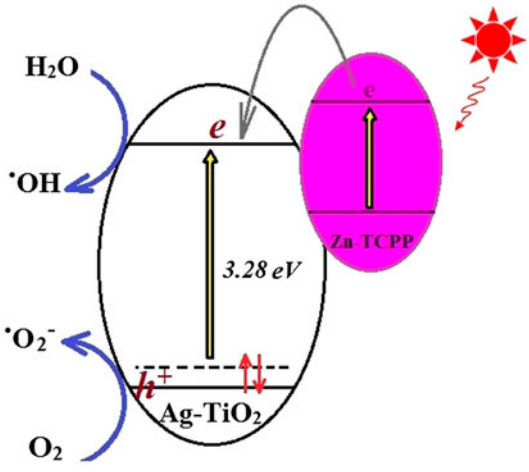

Fig. 9. A possible mechanism to the degradation of pollutants Zn-TCPP/Ag–TiO_2 under visible light irradiation.

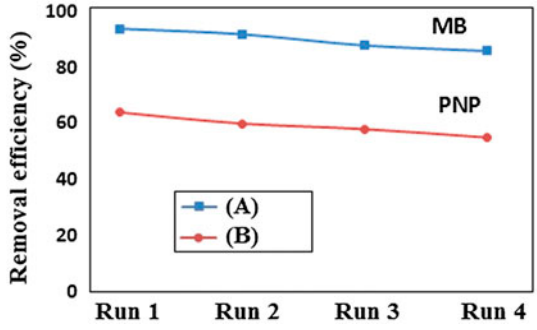

Fig. 10. Reusability of Zn-TCPP/Ag–TiO_2 catalyst for the degradation of (A) MB and (B) PNP (conditions: 50 mL of 5 mg L^{-1} concentrations and 0.05 g catalyst, 90 min).

4. Conclusions

The Zn-TCPP/Ag-doped mesoporous TiO_2 photocatalyst was synthesized using P123 as a surfactant through a sol–gel method for MB and PNP degradation under UV and visible light irradiation. The prepared photocatalysts were characterized by XRD, FT-IR, UV–vis-DRS, XRF, ICP, and SEM images. The XRD pattern shows anatase phases for Ag–TiO_2. The obtained data from UV–vis absorption spectra indicated that through the process of doping Ag with TiO_2, the wavelength of TiO_2 absorption is increased (red shift). On the other hands, immobilizing of porphyrin onto surface of Ag-TiO_2 can raise the photocatalytic activity of it under visible light irradiation. The results of indicated that porphyrin/TiO_2 complexes have significant efficiency of photocatalytic degradation under visible light irradiation. These evidences also reveal that the system of porphyrin/TiO_2 complexes can directly utilize sunlight and can be used to treat organic pollutants in practical wastewater treatment factories.

Acknowledgments

We are grateful to the council of Iran University of Science and Technology for providing financial support to undertake this work.

References

[1] Y. Shaoqing, H. Jun, W. Jianlong, Radiation-induced catalytic degradation of *p*-nitrophenol (PNP) in the presence of TiO_2 nanoparticles, Radiat. Phys. Chem. 79 (2010) 1039–1046.
[2] C.-P. Yu, Y.-H. Yu, Mechanisms of the reaction of ozone with p-nitrophenol, Ozone: Sci. Eng. 23 (2001) 303–312.

[3] M.A. Oturan, J. Peiroten, P. Chartrin, A.J. Acher, Complete destruction of p -nitrophenol in aqueous medium by electro-Fenton method, Environ. Sci. Technol. 34 (2000) 3474–3479.
[4] N. Nasuha, B.H. Hameed, A.T.M. Din, Rejected tea as a potential low-cost adsorbent for the removal of methylene blue, J. Hazard. Mater. 175 (2010) 126–132.
[5] B. Bayarri, J. Giménez, D. Curcó, S. Esplugas, Photocatalytic degradation of 2, 4-dichlorophenol by TiO_2/UV: Kinetics, actinometries and models, Catal. Today 101 (2005) 227–236.
[6] J. Xue, J. Wang, Radiolysis of pentachlorophenol (PCP) in aqueous solution by gamma radiation, J. Environ. Sci. 20 (2008) 1153–1157.
[7] S. Antonaraki, E. Androulaki, D. Dimotikali, A. Hiskia, E. Papaconstantinou, Photolytic degradation of all chlorophenols with polyoxometallates and H_2O_2, J. Photochem. Photobiol. A: Chem. 148 (2002) 191–197.
[8] A.-K. Axelsson, L.J. Dunne, Mechanism of photocatalytic oxidation of 3, 4-dichlorophenol on TiO_2 semiconductor surfaces, J. Photochem. Photobiol. A: Chem. 144 (2001) 205–213.
[9] I. Ilisz, A. Dombi, K. Mogyorósi, A. Farkas, I. Dékány, Removal of 2-chlorophenol from water by adsorption combined with TiO_2 photocatalysis, Appl. Catal. B: Environ. 39 (2002) 247–256.
[10] H.W. Kim, S.H. Shim, Synthesis and characteristics of SnO_2 needle-shaped nanostructures, J. Alloys Compd. 426 (2006) 286–289.
[11] H.W. Kim, J.W. Lee, S.H. Shim, C. Lee, Controlled growth of SnO_2 nanorods by thermal evaporation of Sn powders, J. Korean Phys. Soc. 51 (2007) 198.
[12] A. Mills, S. Le Hunte, An overview of semiconductor photocatalysis, J. Photochem. Photobiol. A: Chem. 108 (1997) 1–35.
[13] D. Tryk, A. Fujishima, K. Honda, Recent topics in photoelectrochemistry: Achievements and future prospects, Electrochim. Acta 45 (2000) 2363–2376.
[14] M.R. Hoffmann, S.T. Martin, W. Choi, D.W. Bahnemann, Environmental applications of semiconductor photocatalysis, Chem. Rev. 95 (1995) 69–96.
[15] Z. Zou, J. Ye, K. Sayama, H. Arakawa, Direct splitting of water under visible light irradiation with an oxide semiconductor photocatalyst, Nature 414 (2001) 625–627.
[16] A. Hagfeldt, M. Grätzel, Molecular photovoltaics, Acc. Chem. Res. 33 (2000) 269–277.
[17] T. Kawahara, Y. Konishi, H. Tada, N. Tohge, J. Nishii, S. Ito, A patterned TiO_2(anatase)/TiO_2(rutile) Bilayer-type photocatalyst: Effect of the anatase/rutile junction on the photocatalytic activity, Angew. Chem. Int. Ed. 41 (2002) 2811–2813.
[18] B. Ohtani, Y. Ogawa, S.-I. Nishimoto, Photocatalytic activity of amorphous-anatase mixture of titanium (IV) oxide particles suspended in aqueous solutions, J. Phys. Chem. B 101 (1997) 3746–3752.
[19] N. Serpone, A. Emeline, Modelling heterogeneous photocatalysis by metal-oxide nanostructured semiconductor and insulator materials: Factors that affect the activity and selectivity of photocatalysts, Res. Chem. Intermed. 31 (2005) 391–432.
[20] M.-Y. Chang, Y.-H. Hsieh, T.-C. Cheng, K.-S. Yao, M.-C. Wei, C.-Y. Chang, Photocatalytic degradation of 2,4-dichlorophenol wastewater using porphyrin/TiO_2 complexes activated by visible light, Thin Solid Films 517 (2009) 3888–3891.
[21] S. Karvinen, The effects of trace elements on the crystal properties of TiO_2, Solid State Sci. 5 (2003) 811–819.
[22] G. Kumara, A. Konno, K. Shiratsuchi, J. Tsukahara, K. Tennakone, Dye-sensitized solid-state solar cells: Use of crystal growth inhibitors for deposition of the hole collector, Chem. Mater. 14 (2002) 954–955.
[23] M.Y. Chang, C.Y. Chang, Y.H. Hsieh, K.S. Yao, T.C. Cheng, C.T. Ho, Photocatalytic degradation of Methylene blue using Porphyrin/TiO_2 complexes activated by visible light, Adv. Mater. Res. 47–50 (2008) 471–474.
[24] X.-S. Feng, S.-Z. Kang, H.-G. Liu, J. Mu, Study of the photophysical properties of composite film assembled of porphyrin and TiO_2 nanoparticles, Thin Solid Films 352 (1999) 223–227.
[25] D. Chen, D. Yang, J. Geng, J. Zhu, Z. Jiang, Improving visible-light photocatalytic activity of N-doped TiO_2 nanoparticles via sensitization by Zn porphyrin, Appl. Surf. Sci. 255 (2008) 2879–2884.
[26] P.-C. Yao, S.-T. Hang, C.-W. Lin, Photocatalytic destruction of gaseous toluene by porphyrin-sensitized TiO_2 thin films, J. Taiwan Inst. Chem. Eng. 42 (2011) 470–479.